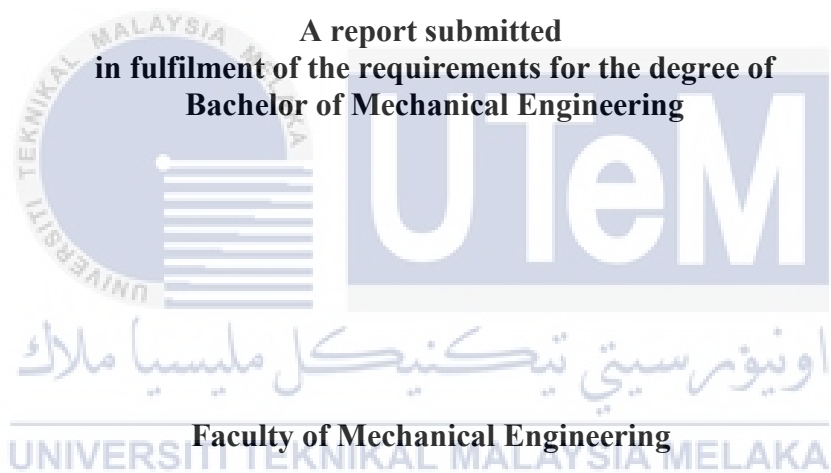


**CFD AERODYNAMICS STUDY OF UNMANNED AERIAL VEHICLE (UAV)
DRONE**

OOI JUN WAI



UNIVERSITI TEKNIKAL MALAYSIA MELAKA

2021

DECLARATION

I declare that this report entitled “CFD Aerodynamics Study of Unmanned Aerial Vehicle (UAV)” is the result of my own work except as cited in the references

Signature :

Name : OOI JUN WAI

Date :



اونيورسيتي تيكنيكل مليسيا ملاك

UNIVERSITI TEKNIKAL MALAYSIA MELAKA

APPROVAL

I hereby declare that I have read this project report and in my opinion this report is sufficient in terms of scope and quality for the award of the degree of Bachelor of Mechanical Engineering.



Signature :

Supervisor's Name : DR. MOHAMAD SHUKRI BIN ZAKARIA

Date :

اوتیورسیٹی ٹیکنیکل ملیسیا ملاک

UNIVERSITI TEKNIKAL MALAYSIA MELAKA

ABSTRACT

The conventional wings of aircraft for Unmanned Aerial Vehicle (UAV) consists of problems such as vortices occurred around the wingtip and also wake region on the upper surface of the wings where these phenomena will greatly reduce the aerodynamic performance of the wings. The present study aims to propose a wing that minimize the drawbacks and offer a better aerodynamic performance with the addition of winglets and vortex generators. The numerical results of the simulation for the clean wing was compared with the experimental results to validate the technique of simulation and the average deviation is only about 4% for the lift-to-drag ratio which showed a great agreement. The behaviour of the fluid flow around the wing was observed, it can be concluded that adding winglets on the wings able to shift the position of vortices and also reduce the magnitude of vortices. On the other hand, adding vortex generators able to reduce the wake region between the fluid and the upper surface of wings. However, by adding the vortex generators will increase the drag of the wings by 5.5%, despite the drawback of generating minimum additional drag, the redesigned wing still able to contribute 15% additional lift. Finally, the optimization for the lift-to-drag ratio considering various length of vortex generators and angle of rotation for vortex generators was performed. The optimized design of wings was able to produce a maximum lift-to-drag ratio of 6.889 at optimal settings of vortex generators length and angle of rotation for vortex generators.

ABSTRAK

Sayap pesawat konvensional untuk Kenderaan Udara Tidak Berawak (UAV) mempunyai masalah seperti pusaran yang berlaku di sekitar hujung sayap dan juga kawasan bangun di permukaan atas sayap di mana fenomena ini akan mengurangkan prestasi aerodinamik sayap. Kajian ini dijalankan bertujuan untuk mencadangkan sayap yang meminimumkan kekurangan dan menawarkan prestasi aerodinamik yang lebih baik dengan penambahan sayap dan penjana pusaran. Hasil numerik simulasi untuk sayap bersih dibandingkan dengan hasil eksperimen untuk mengesahkan teknik simulasi dan itu menunjukkan perbandingan yang baik iaitu penyelewengan sebanyak 4% sahaja bagi nisbah angkat-ke-seret. Tingkah laku aliran cecair di sekitar sayap diperhatikan, dan dapat disimpulkan bahawa menambahkan winglet pada sayap dapat mengubah posisi pusaran dan juga mengurangkan besarnya pusaran. Sebaliknya, menambah penjana pusaran dapat mengurangkan kawasan bangun antara cecair dan permukaan sayap atas. Walau bagaimanapun, dengan menambahkan penjana pusaran akan meningkatkan daya tarikan sayap sebanyak 5.5%, walaupun kekurangan menghasilkan seretan tambahan minimum, sayap yang direka bentuk semula masih dapat menyumbang peningkatan 15%. Akhirnya, pengoptimuman untuk nisbah angkat-ke-seret dengan mempertimbangkan pelbagai panjang penjana pusaran dan sudut putaran untuk penjana pusaran dilakukan. Reka bentuk sayap yang dioptimumkan mampu menghasilkan nisbah angkat-ke-tarik maksimum 6.889 pada tetapan optimum panjang dan sudut putaran penjana pusaran.

ACKNOWLEDGEMENTS

First of all, I would like to express my greatest gratitude to my supervisor Dr. Mohamad Shukri Bin Zakaria from Faculty of Mechanical Engineering, Universiti Teknikal Malaysia Melaka in guiding me throughout the process of research. I am immensely grateful to him for sharing his knowledge in his expertise field and encouragement throughout the duration of this project.

In addition, I would like to thank my parents Mr. Ooi Sung Yen and Mrs. Chung Lai Kuen for their constant support, encouragement and recognition to me.

Last but not least, I would like to thank my classmates Gok Wei Keong and Lee Yik Shern for guiding me through the final year project. I am grateful to have met a group of friends who have always been supportive of me during my time as a university student.

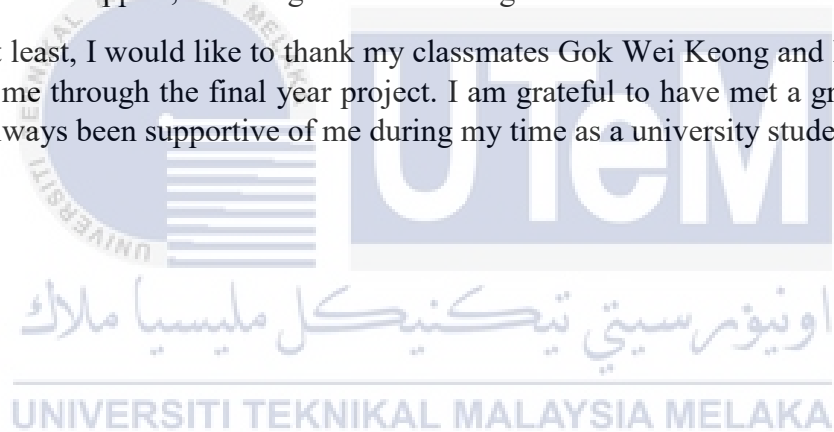


TABLE OF CONTENT

	PAGE
DECLARATION	
ABSTRACT	i
ABSTRAK	ii
ACKNOWLEDGEMENTS	iii
TABLE OF CONTENT	iv
LIST OF FIGURES	vi
LIST OF TABLE	viii
LIST OF SYMBOL	ix
CHAPTER	
1. INTRODUCTION	
1.1 Background	1
1.2 Problem Statement	3
1.3 Objective	4
1.4 Scope of Project	5
2. LITERATURE REVIEW	
2.1 Vortex Generator	8
2.2 Aerodynamic Analysis of UAV	9
2.3 Winglet Optimisation of UAV	13
2.4 Experimental Study of UAV	16
2.5 Summary	18
3. METHODOLOGY	
3.1 Introduction	19
3.2 Geometric Model (Reference)	21
3.3 Boundary Condition	23
3.4 Meshing Strategy	24
3.5 Governing Equation	26
3.6 Numerical Model	28
3.7 Central Composite Design (CCD)	29
4. RESULT	
4.1 Introduction	32
4.2 Grid Independence Test	33
4.3 Model Validation	35
4.4 Pressure Contours and Velocity Contours of the Wing in Different AoA (α)	38
4.5 Vortices Around the Wingtip	41
4.6 Flow Field Observation	44
4.7 Optimization	49
5 CONCLUSION AND RECOMMENDATIONS	57



LIST OF FIGURES

FIGURE	TITLE	PAGE
1.1	UAV funding profile	2
1.2	Base Line Vortex Generator off	4
1.3	Static Pressure Coefficient and Streamlines in the Vortex Core	4
2.1	Definition of vane-type passive VG devices	7
2.2	Definition of wheeler-type vortex generator	7
2.3	Lift coefficient versus angle of attack by Datcom method	10
2.4	Drag Coefficient versus angle of attack by Datcom method	12
2.5	Whitcomb's winglet design	15
2.6	Definition of the basic winglets angle	16
2.7	Test boom Installation	17
3.1	The Methodology Flowchart	20
3.2 a)	Profile of NACA 65(3)-218	21
3.2 b)	Drawing of the wing	21
3.2 c)	Drawing of redesigned wing	22
3.2 d)	Computational domain	22
3.3	Computational domain and Schematic drawing of wing	24
3.4 a)	Face sizing of wing	25
3.4 b)	Face sizing of VGs	25
3.5	Inflation layers around the wing	26
4.1	Graph of Drag Coefficient, at AOA 0° vs Number of Cells	34
4.2	Graph of Lift Coefficient (C_L) vs AOA (α) at Re number 2.5×10^5	36
4.3	Graph of Lift Coefficient (C_D) vs AOA (α) at Re number 2.5×10^5	36
4.4	Graph of Lift to Drag Ratio (L/D) vs AOA (α) at Re number 2.5×10^5	37
4.5 a)	Pressure Contour of Wing for AoA= 0°	38

4.5 b)	Velocity Contour of Wing for AoA=0°	38
4.6 a)	Pressure Contour of Wing for AoA=4°	39
4.6 b)	Velocity Contour of Wing for AoA=4°	39
4.7 a)	Pressure Contour of Wing for AoA=8°	40
4.7 b)	Velocity Contour of Wing for AoA=8°	40
4.8	Plane located at the different section of the wing at AoA $\alpha=4^\circ$	41
4.9 a)	Vortices around wingtip at the leading edge at AoA 4°	42
4.9 b)	Vortices around wingtip at the mid-section at AoA 4°	42
4.9 c)	Vortices around wingtip at the trailing edge at AoA 4°	43
4.10	Geometry of Wing with Winglet and Vortex Generator at $\alpha=8^\circ$	44
4.11 a)	Vorticity occur around the wingtip AoA=8° (Re=2.5×105) [Clean Wing]	45
4.11 b)	Vorticity occur around the winglet at AoA=8° (Re=2.5×105) [Redesigned Wing]	45
4.12 a)	Streamlines around mid-section at AoA=8° (Re=2.5×105) [Clean Wing]	46
4.12 b)	Streamlines around mid-section at AoA=8° (Re=2.5×105) [Redesigned Wing]	47
4.13 a)	3D Streamlines around the wing at AoA=8° (Re=2.5×105) [Clean Wing]	48
4.13 b)	3D Streamlines around the wing at AoA=8° (Re=2.5×105) [Redesigned Wing]	48
4.14	Isometric view of wing	50
4.15	Length of VGs, l	50
4.16	Angle rotation of VGs, β	51
4.17	Height of VGs, H	51
4.18	Spacing between VGs, λ	52
4.19	Table of Analysis of Variance (ANOVA)	53
4.20	Graph of multiple response prediction.	54
4.21	Surface Plot of L/D vs X2 β , X1 l	55
4.22	Optimized geometry of VGs on wing	56

LIST OF TABLES

Table	Title	Page
1.1	UAVs Classification according to the US Department of Defense (DoD)	1
2.1	Drag Distribution between the different parts of the HCUAV	14
3.1	The geometric parameters of reference wing	23
3.2	Face Sizing Setting	25
3.3	Inflation setting	26
3.4	A Central Composite Design with three-level, two factor factorial design	31
4.1	Summary of grid independence test	33
4.2	Data of Simulation Results and Experimental Results	35
4.3	Comparison of coefficients between configuration I and II	49
4.4	Design of experiment	53

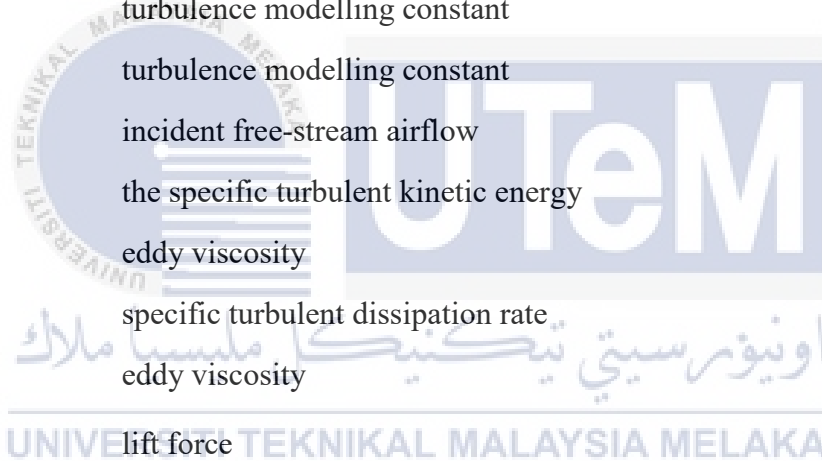
UNIVERSITI TEKNIKAL MALAYSIA MELAKA

LIST OF SYMBOLS

UAV	Unmanned aerial vehicles
AGL	Above ground level
MSL	Median sea level
C_L	Lift Coefficient
C_D	Drag Coefficient
L/D	Lift to drag ratio
AoA	Angle of attack
CFD	Computational Fluid Dynamics
ANSYS	Analysis System
VG	Vortex generator
Re	Reynolds number
RANS	Reynolds-averaged Navier–Stokes equations
u	flow velocity
u_g	grid velocity
ρ	density
\emptyset	property of the fluid
dA	surface area of the fluid domain
Γ	diffusion coefficient
S_φ	source term of φ
∂V	boundary of the control volume
V	control volume
LES	Large eddy simulation
$C_{L\alpha}$	Lift curve slope

K_N	Ratio of the nose lift to wing alone lift
$K_{W(B)}$	Ratio of the wing lift in presence of the body, to wing alone lift
$\frac{S_{We}'}{S'}$	Ratio of wetted area of the exposed wing to gross planform areas of the fore surface
$(C_{L\alpha})_e$	Lift curve slope of exposed wing
$\overline{\delta\varepsilon}$	Downwash derivative
$\frac{\delta\alpha}{q''}$	Average dynamic pressure ratio acting on the aft surface
$\frac{q_\infty}{q_\infty}$	
$\frac{S''}{S'}$	Ratio of aft to forward gross planform areas
$\frac{S_e''}{S''}$	Ratio of the exposed to gross planform areas of the fore surface
(C_{L0})	Zero-angle of attack lift coefficient
i_w	Wing setting angle
α_{0w}	Zero-lift angle of attack of wing
$(C_{L\alpha})_e$	Lift curve slope of exposed wing
α_0	Zero-lift angle of attack
$(C_{L\alpha})_w$	Lift curve slope of wing
$(C_{Lmax})_{WB}$	Wing-Body maximum lift coefficient
L	Airfoils thickness location parameter
$\frac{t}{c}$	Average stream wise thickness ratio of the wing
R_{LS}	Lifting surface correction factor
S_{wet}	Wetted area
S_{ref}	Reference area
$\frac{l_B}{d}$	Body fineness ratio
C_{D0}	Zero lift-Drag
C_f	flat plate skin friction coefficient
$(C_{D0})_P$	zero lift drag coefficient of tail panel

$(C_{Do})_H$	zero lift drag coefficient of horizontal tail panel
$(C_{Do})_V$	zero lift drag coefficient of vertical tail panel
KARI LWST	Korea Aerospace Research Institute Low Speed Wind Tunnel
V_a	Free-stream velocity
L_R	Reference length
SST	Menter's shear stress transport
C	Chord Length
Pa	Pascal
y^+	Non-dimensional boundary layer distance
\bar{P}_k	rate of production k
β^*	turbulence modelling constant
σ_k	turbulence modelling constant
U	incident free-stream airflow
k	the specific turbulent kinetic energy
μ_k	eddy viscosity
ω	specific turbulent dissipation rate
μ_ω	eddy viscosity
L_F	lift force
D_F	drag force



CHAPTER 1

INTRODUCTION

1.1 Background

Unmanned aerial vehicles (UAV) are defined as aircraft that do not require any human crew to fly. There are two method of flying UAVs which is fully autonomous or being remotely controlled by a human pilot. The size of the UAVs ranging from a palm-size to a large size which is comparable to a jet fighter, while the weight, normal operating altitude, and airspeed can be classified into different categories (Table1.1).

Table 1.1 UAVs Classification according to the US Department of Defense (DoD)

Category	Size	Maximum Gross Takeoff Weight (MGTW) (lbs)	Normal Operating Altitude (ft)	Airspeed (knots)
Group 1	Small	0-20	<1200 AGL	<100
Group 2	Medium	21-55	<3500	<250
Group 3	Large	<1320	<18000 MSL	<250
Group 4	Larger	>1320	<1800 MSL	Any airspeed
Group 5	Largest	>1320	>1800	Any airspeed

In recent years, there has been a significant growth of interest in the research of UAVs as indicated by the increase of numbers for the conferences and journals contributed on plenty different aspects ranging from aerodynamics, flight performance, stability, and control (Arshad, 2010). According to (Bolkcom, 2003), the future trend of aircraft will bring

focus from manned to unmanned aerial vehicles shown in Figure 1.1. It is convinced that funding for UAVs will be tripled, holding out over 10 billion dollars in the current decade.

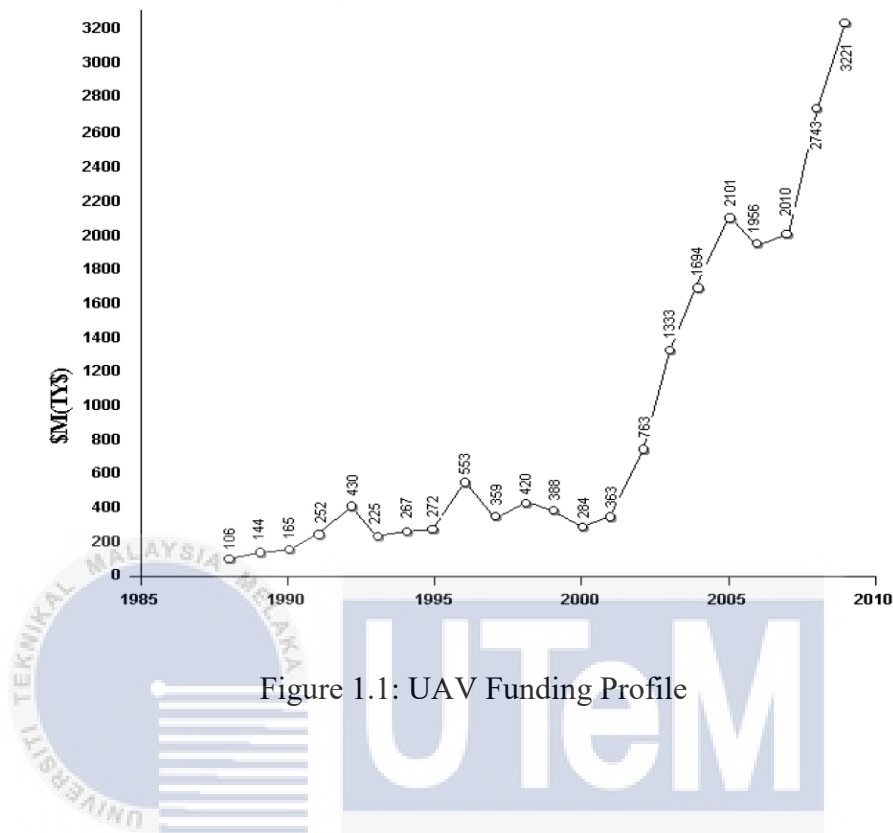


Figure 1.1: UAV Funding Profile

Besides, the advantage of UAVs is the flight endurance of UAVs will not limited by the endurance of the pilot especially the “g” force exerted on the on-board crew. Additionally, according to the statements mentioned which make UAV a great option for military force to undergo missions involving a high degree of risk as the cost of operating a UAV is greatly reduced compare to a manned aircraft, missions such as visual identification, laser nomination of targets and bomb damage execution in enemy territory and electronic deception can be executed without putting any lives and costly aircraft into risk. UAVs are generally difficult to be detected using radar or infrared systems consequence by the small size, low noise and speed.

Due to the rapid development of technologies, it is believed that UAVs can diversify its application to the other region such as logistics, geology, agriculture, and

transportation. Therefore, it is crucial to optimize the flying and aerodynamic performance in order to involve UAVs in other regions.

1.2 Problem statement

The conventional wings of aircraft have a common problem of vortices occurred around the tip of wings due to the fluid move in circular motion, which the higher pressure side with low velocity of air will flow to the lower pressure side with high velocity air flow caused a formation of vortices (Figure 1.3) at the tip of wing. However, this phenomenon is necessary in order to generate sufficient lift force. On the other hand, when an aircraft is cruising, the friction between the air and the wall reduce the kinetic energy of the boundary layer formed between the surface of the wing and air. When this happen, the boundary layer formed will be separated from the surface (Figure 1.2) of the wing and creates a wake region causing a pressure difference and induced a high drag force. These problems will increase the fuel consumption of the UAVs and decrease the range of flight. Moreover, the induced drag on the wingtip is overwhelmed it may cause damage on the wing consequence safety risks during the flight.

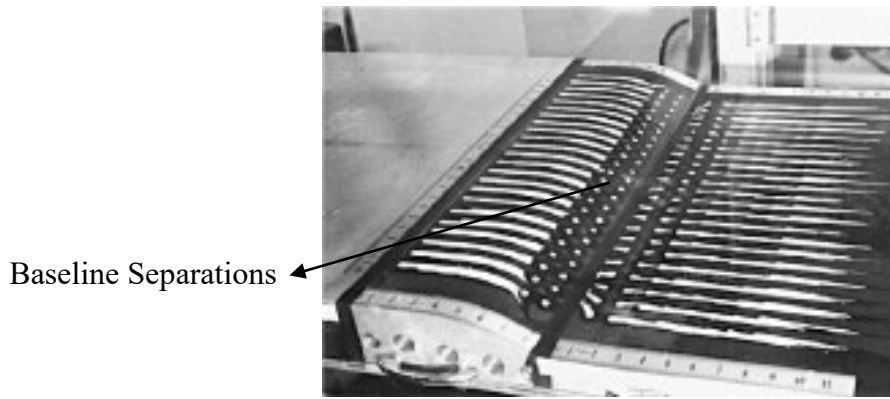


Figure 1.2 Base Line Vortex Generator off case source from (Lin, 2002).



Figure 1.3 Static Pressure Coefficient and Streamlines in the Vortex Core source from (Jean, *et. al*, 2016)

1.3 Objectives

The aims of this projects are as following:

- i. To develop CFD model of flow characteristic around the wing of UAV.
- ii. To optimize the length (L) and angle of rotation (β) of vortex generators under the constraint of fixed parameters winglet and propose a redesigned wing.
- iii. To compare the lift coefficient (C_L), drag coefficient (C_D), and lift-to-drag (L/D) ratios with an angle of attack (AoA) of clean wing and redesigned wing using CFD.

1.4 Scope of project

The scopes of this projects are:

- i. Results of the simulation are presented in this report and only bounded around the wings of the UAV.
- ii. Results of the simulation are simulated using ANSYS and validated using the results of past experimental research.
- iii. The Re number and the AoA is 2.5×10^5 and 8° respectively for the results of optimization.



CHAPTER 2

LITERATURE REVIEW

2.1 Vortex Generator

There are few techniques can be used to control the flow of fluid around the wing of the UAV, one of the passive flow control is vortex generator (VG). Vortex generators able to enhance the aerodynamics performance of the aircraft in the condition of cruising and maneuver. At a subsonic condition which also consider as low Reynolds number (Re), the boundary layer of the flow is stable overall while the existence of an adverse pressure gradient cause a laminar separation. Without the disturbance results in externally force, the phenomena of the separation of laminar can elongate to the trailing edge of the aerofoil, a large pressure drag on the aerofoil will occur (Stack and Mangalam, 1990). Vortex Generators have been widely applied to dynamize the boundary layers which are “sluggish”, which are generally turbulent and thick. The purpose of vortex generators is to detain the separation and results in increasing the maximum lift coefficient. The vortex generators are usually a small inclined vane which may be in rectangular or triangular shapes. The working principle of the vortex generator is by mixing the high-energy freestream fluid into the lower magnitude of the boundary layer, therefore to energize it. The size of the vortex generators is usually designed according to the half of the height of the boundary-layer thickness (Kerho, 2003). However, vortex generators do have drawbacks, they generate minimum of drag penalty and may reduce the maximum lift-to-drag ratio. Despite the drawbacks, vortex generators are able to increase the maximum lift coefficient and extend the angle of attack

of stall (Bragg and Gregorek, 1987). Vortex generators were also analysed and found to enhance the degenerated performance consequent by the trip strip back to the “clean section” level. The drag penalty can be reduced better by wheeler-type vortex generators (Figure 2.2) than the typical vortex generators for the similar levels of flow control (Barrett and Farokh, 1993).

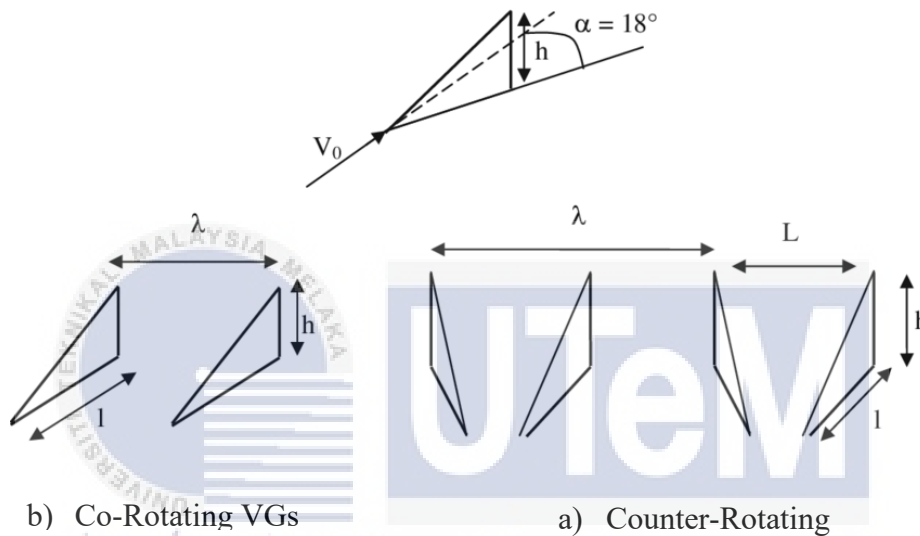


Figure 2.1 Definition of vane-type passive VG devices (Bur, 2009)

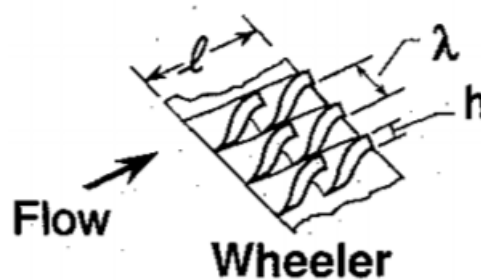


Figure 2.2 Definition of wheeler-type vortex generator (Lin, 1990)

Few parametric studies have been conducted by several researchers, Godard, 2006, Pauley and Eaton, *et al*, 1998 and Ahmad, *et al*, 2005. the results show that skewed angle of vortex generator will affect the skin friction and vortices magnitude downstream of the

vortex generator. In the other hand, the spacing between each couple of vortex generators have been tested by Ahmad and Bur, *et al.* The other researchers also tested and analysed the effects of follow control in Sub-vortex generators, micro-vortex generators and blowing-vortex generators (Lin, 1999), (Babinsky, *et al.*, 2007) and (Jiang, *et al.*, 2012). The drag reduction can be increased by a relatively low height vortex generator as it can produce a preferable eddy structure without prematurely generating a downstream turbulent boundary layer. In fact, it is also observed that the mutual vortex interference which leads to a faster vortex decay can be decreased by increasing the gap ratio of the counter rotating vanes (see figure 2.1 for the definition of vane-type VG devices), besides, the device can be prevented from adversely affecting the boundary layer in adverse pressure gradient flow (Lin, 2002).

The flow phenomenon above the airfoil with and without vortex generators has been studied by using the computational fluid dynamics (CFD), as it can easily design the most optimized flow devices. The CFD simulation results showed that it is effective in reattaching the split shear layer and decreasing the size of separation zone by applying passive vortex generator (Shan, *et al.*, 2005). The governing equation of CFD code FLUENT 6.3™ compressible (RANS) is as following:

$$\frac{d}{dt} \int_V \rho \phi dV + \int_{\partial V} \rho \phi (u - u_g) dA = \int_{\partial V} \Gamma \nabla \cdot dA + \int_V S_\phi dV \quad (2.1)$$

where u is the flow velocity vector, u_g the grid velocity of the moving meshes, ρ the density of fluid, ϕ the property of the fluid and dA the surface area of the fluid domain under consideration. The term Γ represents the diffusion coefficient and S_ϕ represents the source term of ϕ . The term ∂V is used to represent the boundary of the control volume V . In fact, the RANS model able to provide a decent value even the coarser grid has been applied compared to the common LES models which could not provide an acceptable value (Johansen, *et al.*, 2004)

2.2 Aerodynamic Analysis of UAV

In the initial design of an aircraft, the estimation of the aerodynamic characteristics of aircraft, there are several ways of obtaining the characteristics of the aircraft such as wind tunnel testing, smoke, tufts, laser sheet and surface oil flow. However, for the different design, plenty of new tests will be needed to carry out and this will be a time wasting action. From the statement mentioned the cost of design will be surged up. Therefore, computational fluid dynamics (CFD) simulation is a better option and more convenient way to estimate the aerodynamic characteristics (Haris and Md Nizam, 2008).

The method for the calculation of the subsonic, transonic and supersonic derivatives are provided in the Datcom method which is a USAF stability and control handbook. In order to use Datcom method to estimate the lift coefficient (C_L), it is mandatory to determine few aerodynamic characteristics using the following equations,

$$C_{L\alpha} = (C_{L\alpha})_e [K_N + K_{W(B)} + K_{B(W)}] \frac{S_{We'}}{S'} + (C_{L\alpha})_e [K_{W(B)} + K_{B(W)}]''' [1 - \frac{\delta\epsilon}{\delta\alpha}] \frac{q''}{q_\infty} \frac{S''}{S'} \frac{S_e''}{S''} \quad (2.2)$$

$$(C_{L0}) = [i_W - (\alpha_{oW})](C_{L\alpha}) \quad (2.3)$$

In order to determine the lift coefficient, the aerodynamics properties for the parts following must be established, such as wing-body, wing alone, body alone, and tail alone. These properties are: α_o , $(\alpha_o)_W$, $(C_{L\alpha})_e$, $(C_{L\alpha})_w$, $(C_{L\alpha})_{WB}$, $(\alpha C_{Lmax})_W$, $(\alpha C_{Lmax})_{WB}$, $(C_{Lmax})_{WB}$

The wing-body-tail lift curve slope and zero-angle-of-attack lift coefficient can be obtained by using equation (2.2) and (2.3). While by combining eq. (2.2) and eq. (2.3) the lift coefficient of wing-body and tail combination that various with angle of attack can be estimated (Douglas, 1978).

$$(C_L) = (C_{L0}) + (C_{L\alpha})\alpha \quad (2.4)$$

In figure 2.3, the value of C_{Lmax} from the calculation equation (2.5) yielded 1.467 for the wing-body combination as well as the wing alone, which means that the aerodynamics effects of the fuselage were negligible by referring to the equation (2.6). In the other hand, base of figure 2.3 it shows that the wing body combination has lift coefficient higher than wing body tail combination which consequence by the involvement of tail panels. According the eq. (1), the tail inference which gave the negative value referred by the second term, while the curve slope for wing body combination referred by the first term. When the both terms are being summed up, it will result a lower value than the wing body combination.

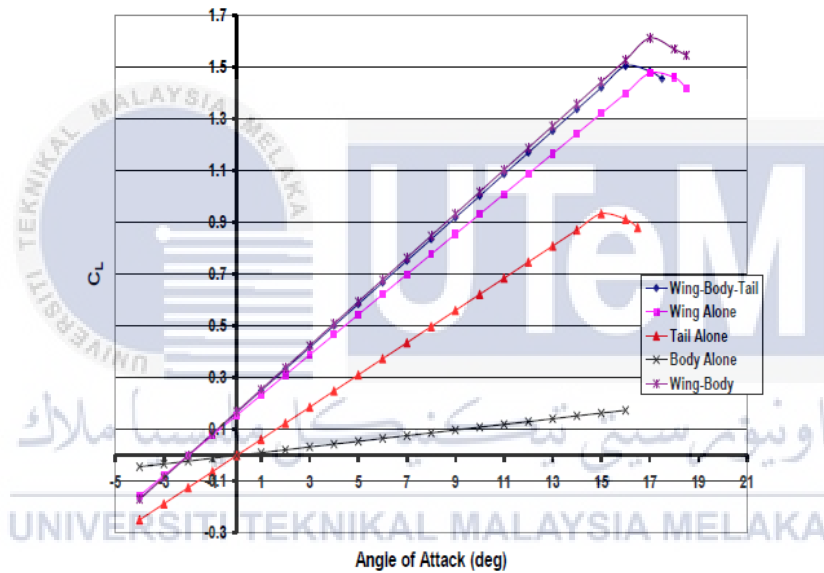


Figure 2.3 Lift coefficient versus angle of attack by Datcom method

$$\begin{aligned}
 C_{L\alpha} &= (C_{L\alpha})_e [K_N + K_{W(B)} + K_{B(W)}] \frac{S_{we}}{S} + \\
 &(C_{L\alpha})_e [K_{W(B)} + K_{B(W)}] \left[1 - \frac{\bar{\delta}\epsilon}{\delta\alpha} \frac{q''}{q_\infty} \frac{S''}{S'} \frac{S_e''}{S''} \right] \\
 (C_{L0}) &= [i_w - (\alpha_{0W})] (C_{L\alpha}) \\
 (C_L) &= (C_{L0}) + (C_{L\alpha}) \alpha
 \end{aligned} \tag{2.5}$$